LAL 00-67
November 2000

PERFORMANCES OF THE NA48 LIQUID KRYPTON CALORIMETER

Guillaume Unal*
LAL, IN2P3-CNRS et Université Paris-Sud, BP.34, 91898 Orsay, France

ABSTRACT

The NA48 experiments aims at a precise measurement of direct CP violation in the neutral Kaon system. This puts stringent requirements on the electromagnetic calorimeter used to detect photons of average energy 25 GeV. The choice of NA48 is a quasi homogeneous Liquid Krypton calorimeter with fast readout. The operation of this device and the performances achieved are described.

1 Introduction

The NA48 experiment at the CERN SPS aims at a precise measurement of the ϵ'/ϵ parameter, characterising direct CP violation in the neutral kaon decays.

*on behalf of the NA48 collaboration (Cagliari, Cambridge, CERN, Dubna, Edinburgh, Ferrara, Firenze, Mainz, Orsay, Perugia, Pisa, Saclay, Siegen, Torino, Warsaw, Wien)

This parameter can be accessed experimentally through the double ratio R of the decay rates :

$$R = \frac{\Gamma(K_L \to \pi^0\pi^0)/\Gamma(K_S \to \pi^0\pi^0)}{\Gamma(K_L \to \pi^+\pi^-)/\Gamma(K_S \to \pi^+\pi^-)} \approx 1 - 6 \times Re(\epsilon'/\epsilon) \qquad (1)$$

To achieve the required accuracy of $\approx 2\times10^{-4}$ on ϵ'/ϵ, a large statistic is needed. To minimise systematic effects, NA48 collects the four modes at the same time using simultaneous K_L and K_S beams and from the same decay region, such that most effects cancel at first order in the double ratio. A description of the analysis of the data taken in 1997 can be found in [1].

The $\pi^0\pi^0$ decay mode is identified by measuring four photons in the calorimeter, in the energy range 3-100 GeV, with an average energy of ≈ 25 GeV. The calorimeter is located ≈ 100 m downstream of the decay region. Photon angles are not directly measured and therefore the distance D between the kaon decay point and the calorimeter is computed assuming the Kaon mass for the four photons, and using the measured photon energies and positions transverse to the beam axis :

$$D \quad = \quad \sqrt{\Sigma_{i>j} E_i E_j [(x_i - x_j)^2 + (y_i - y_j)^2]}/M_K$$

The fiducial decay region is defined by applying cuts on the reconstructed value of D. This decay region should be defined identically for neutral and charged decays and this implies a good control of systematic effects in measuring photon energies and positions. The invariant masses of the two photon pairs are then computed using D and compared to the nominal π^0 mass to select $K_{L,S} \to \pi^0\pi^0$ candidates. To achieve a good rejection of the $K_L \to 3\pi^0$ background (whose decay rate is ≈ 200 times higher than the CP violating $K_L \to \pi^0\pi^0$ mode), a π^0 mass resolution of ≈ 1 MeV is required. In addition, NA48 is using proton tagging to distinguish K_L and K_S decays : the time of each proton directed towards the K_S production target is recorded and compared to the decay time measured in the detector. If a coincidence is found the event is classified as K_S, otherwise it is classified as K_L. This requires a very reliable measurement of the event time with a good (better than 500 ps) resolution.

The requirements on the performances of the calorimeter can be summarised as follows :

1) Energy resolution : should be better than 1% at 25 GeV and above, with

a good uniformity over the calorimeter (long range variations not exceeding $\approx 0.1\%$)
2) Position resolution : of the order of 1 mm
3) Time resolution : better than 500 ps
4) Non linearity : residual non linearities should be understood at the level of 0.1% in the energy range 3-100 GeV
5) Stability : The calorimeter should give a stable response over several years, in a high rate of Kaon decays (the K_L decay rate seen by the detector is $\approx$ 500 kHz)

To fulfil these goals, NA48 has decided to use a quasi homogeneous Liquid Krypton calorimeter, operated as ionization calorimeter. This calorimeter is almost fully active, which ensures a very good intrinsic energy resolution. The use of cold noble liquid allows a very good stability of the response. Initial current readout technique with a fast shaping allows to operate in a high rate environment and to achieve a good time resolution.

Table 1 summarises the characteristics of noble liquids. Clearly, liquid Argon is not dense enough for a homogeneous calorimeter. Xenon would offer a smaller radiation length than Krypton, but its Moliere radius, giving the transverse size of showers, which is in our case a more important parameter, is in fact close to the one of the Krypton. Liquid Krypton was therefore chosen as medium. The calorimeter is briefly described in the next section. The reconstruction of pulses and showers are then described with the performances achieved, with emphasis on the energy resolution and the linearity.

Table 1: *Summary of noble liquid characteristics.*

	Z	density (g/cm^3)	X0 (cm)	R(Moliere) [2] (cm)
Ar	18	1.4	14.0	9.2
Kr	36	2.4	4.7	6.1
Xe	54	3.0	2.9	5.5

2 The Liquid Krypton calorimeter

2.1 Calorimeter structure

The calorimeter is made of a bath of ≈ 10 m^3 of liquid krypton at 120 K with a total thickness of 125 cm ($\approx$ 27 radiation lengths) and a octagonal shaped

active cross-section of ≈ 5.5 m^2. A 8 cm radius vacuum tube goes through the calorimeter to transport the undecayed neutral beam. Thin Copper-Beryllium ribbons (of dimensions 40μm $\times$ 18 mm $\times$ 127 cm) stretched between the front and the back of the calorimeter form a tower structure readout. The 13212 readout cells each have a cross-section of $\approx 2\times2$ cm^2 and consist (along the horizontal direction) of a central anode (at the high voltage) in the middle of two cathodes (kept at the ground). The gap size d is therefore ≈ 1 cm. There is a 2 mm vertical separation between the electrodes. The drift of the ionization electrons towards the anode produces a current i which in the limit of uniform ionization across the gap and constant electric field can be written as :

$$i(t) = q \times \frac{v_d}{d} \times (1 - \frac{t}{t_d}) \tag{2}$$

where q is the charge one wants to measure, v_d the drift velocity [1] and t_d the total drift time across the gap[2]. To guarantee a good uniformity of the initial current ($i(t = 0)$), a good accuracy of the gap is required. This is enforced by the use of five precisely machined spacer plates (fibreglass reinforced epoxy, 5mm thick, ≈ 0.025 X0), normal to the detector axis and located every 21 cm. The spacer plates guide the ribbons in a accordion geometry with a $\pm$ 48 mrad zig-zag angle, in the horizontal direction. Configurations where the shower core is aligned with an electrode, resulting in a drop of the response, are thus avoided. The accuracy achieved in the position of the holes in the spacer plates and therefore in the gap size is typically $\pm$ 45 μm. The overall tower structure is projective towards the middle of the Kaon decay region, which is located $\approx$ 114 m upstream of the calorimeter. The measurement of photon positions becomes thus independent of fluctuations in the longitudinal shower development. Because of the projectivity, the gap size is increasing by 1% between the front and the back of the calorimeter. Figure 1 shows the electrode structure of one quarter of the calorimeter.

The calorimeter is housed in a vacuum insulated cryostat. The warm windows are made of aluminium foil 4mm thick followed on the beam entrance side by a cold double walled stainless window. The outer wall which holds the pressure is convex and 2.9 mm thick, the inner is flat and only 0.5 mm thick. A light honeycomb aluminium structure connects the two foils. The total

[1] typically 3100 m$\cdot$s^{-1} for a high voltage of 3000 V

[2] typically 3.2μs

amount of matter before the beginning of the liquid krypton volume is ≈ 0.8 X0 including all the NA48 detector elements upstream of the calorimeter, out of which ≈ 0.63 X0 comes from the cryostat and the calorimeter itself. Krypton evaporates continuously at the top of the cryostat and flows through an external purifier to be subsequently recondensed and returned to the cryostat. The krypton purity is such that the lifetime of secondary electrons exceeds 100 μs (to be compared to a shaping time of $\approx$ 70 ns). Long term temperature variations within the calorimeter are $< \pm 0.3$ K, with negligible influences on the calorimeter performances.

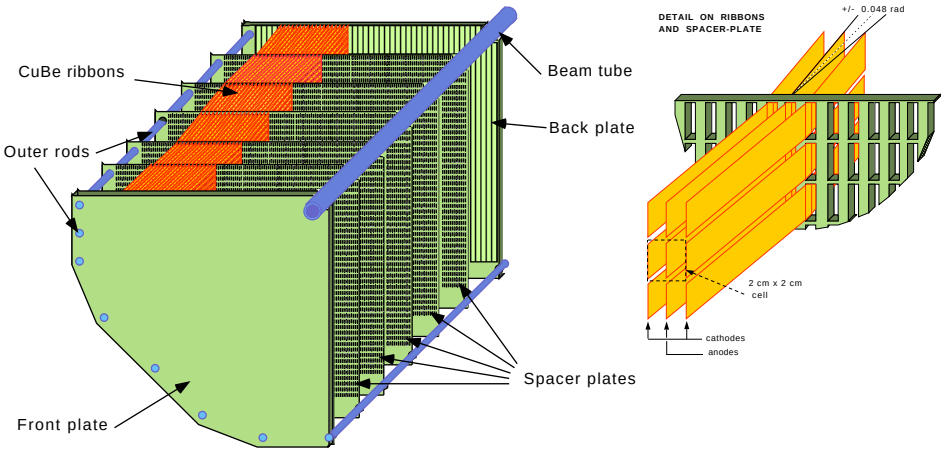

Figure 1: *Electrode structure of one quarter of the calorimeter (left) and details on ribbons and one spacer plate (right).*

2.2 Electronics

Preamplifiers are located on the back plane of the electrode structure. A dual hybrid version of cold charge integration preamplifier, of BNL type using silicon JFET technology, was designed [3]. The restoring time chosen is 150 ns. The output signal from the preamplifiers travels in 6 m long coaxial cables to the feed-throughs. Transceiver boards [4] are mounted directly on the warm side of

the feed-throughs. They perform pole-zero compensation (to restore the quasi ideal triangular shape of the signal, with a rise time of $\approx$ 22 ns), amplification and drive differential output to the digitising electronics via 10 m long shielded twisted pairs cables. The last stage of the electronics [5] performs the final shaping of the signal using a Bessel filter. The shape of the pulse after this filter is almost symmetrical with a width of 70 ns, risetime of 43 ns and a fall time of 52 ns, with an undershoot of $\approx$-3% of the maximum lasting during the total drift time ($\approx$ 3.16 μs). This signal is fed to a gain switching amplifier, where the gain choice is based on the signal before shaping, and then to a 10 bit 40 MHz flash ADC. The event times are asynchronous with the clock frequency. Four gains are used with relative values of 1,2.86,6.89 and 16.80, allowing to cover the energy range $\approx$ -1.5 GeV to 55 GeV per channel. In the highest gain, the sensitivity is $\approx$ 3.5 MeV/count. The total electronic noise per channel (dominated by the preamplifier noise) is $\approx$ 10 MeV. The total dispersion of the gains of the electronic chain from channel to channel is around 3%. The shaped pulse is also used as input of the trigger system [6].

The response uniformity and stability of the full electronic chain is controlled by a calibration system. Calibration pulses are produced locally in the liquid Krypton so as not to suffer from distortion or cross-talk dues to long transmission lines. The generator produces a step of injected current followed by an exponential decay. The amplitude of the signal is given by a reference voltage V controlled by a 15 bit DAC. The injected current can be written as $i = \kappa \times V$, where the constant κ depends on the individual components of the calibration circuit. The intrinsic dispersion of κ is several percent. To achieve a good calibration accuracy, κ was measured for each channel on a test bench, by equalising the calibration signal, produced for a given DAC value, to the signal obtained by directly injecting a calibrated current. The injected current is generated via an external high precision resistor. The ratio of these two calibrations gives the calibration constant κ, expressed in mA/V. These constants were measured at the level of $\approx$ 1% accuracy, for each channel, at room temperature and at 120 K. The technique used simulates the behaviour of the real physics pulses, including the attenuation due to the HV decoupling capacitor, the capacity of the cell, and the capacitive coupling of adjacent cells.

2.3 Calorimeter Operation

The calorimeter assembly has been completed in 1996 when test data with part of the readout electronic were taken. The calorimeter was fully operational in 1997 for the first data taking period for the ϵ'/ϵ measurement. During these two years, the calorimeter had to be operated at a high voltage of 1500 V, lower than expected, because of problems with a small fraction of the blocking capacitors. This led to a small space charge effect from accumulation of positive ions in the gap, distorting the electric field [7]. In the winter 1997/1998, all the blocking capacitors were replaced. This allowed to operate the calorimeter at a high voltage of 3000 V, reducing the space charge effect to a negligible level, and allowing a noise reduction of $\approx 25\%$ (thanks to the higher drift velocity). In 1998,1999 and 2000, data were taken with this configuration. Typically, there are ≈ 50 faulty channels (out of ≈ 13000 in the calorimeter). 30 of those are dead preamplifiers in the liquid krypton. This small mortality happened when the calorimeter was cooled down in 1998. This number has been very stable since, the calorimeter being always kept cold and full of krypton.

3 Pulse reconstruction

For each channel readout, the information of 10 ADC samples is available. The timing is adjusted such that the first two samples are before the beginning of the triggered signal. They can therefore be used to perform a baseline check to determine if the pulse sits on the undershoot of a out-of-time shower. If this is the case, the corresponding baseline is subtracted. The gain choice is done typically 2 time samples before the maximum of the signal and the same gain is kept for five or more time samples. Thus usually, the same gain value is used for all the samples needed to reconstructed the pulse. The pulses are converted to energy using a linear relation $s = g_{gain} \times (\text{ADC-Offset}_{gain})$ derived from calibration events. From this calibrated pulse, the energy (E) and time (T) of the signal are reconstructed using a digital filter method :

$$\begin{aligned} E &= \Sigma a_i \times s_i \\ T &= \frac{1}{E}\Sigma b_i \times s_i \end{aligned} \tag{3}$$

where s_i is the sampled calibrated pulse, and a_i and b_i are digital filter coefficients, derived from the measured pulse shape in calibration events. These

coefficients are binned as a function of the time of the signal, and one iteration is performed to measure both E and T. To improve the accuracy of the procedure, the channels are divided into 10 categories according to the observed pulse width, and coefficients are computed for each category. In calibration events, the pulse reconstruction accuracy is $\approx 0.1\%$ on the energy and $<$150 ps on the time (for high enough signals such that the noise becomes negligible). Three time samples centred around the maximum are used to perform this digital filter computation. This is a compromise between noise reduction and sensitivity to accidental showers. The sample immediately after a gain change is not well measured and in a small fraction of the cases only two samples can be used to reconstruct energy and time.

4 Shower reconstruction

4.1 Shower size

In this quasi-homogeneous calorimeter, with a Moliere radius of $\approx$ 6.1 cm, the dominant intrinsic fluctuations in the energy measurement come from fluctuations in the energy loss outside the finite calorimeter area used to measure the shower. To illustrate the importance of this effect, the expected resolution from the GEANT 3.21 [8] Monte-Carlo program can be computed for various dimensions of the area used to collect the energy. For an infinite size, the "sampling" term would be $\approx 1.2\%/\sqrt{E}$. Using a R=11 cm radius, this increases to $\approx 2.8\%/\sqrt{E}$, and $\approx 3.5\%/\sqrt{E}$ for a 7 cm radius. The size used is a compromise between the electronic noise (which increases with R) and the sampling term (which decreases with R). The value used is R=11 cm, which contains $\approx$ 100 calorimeter cells. This value is kept constant with energy in order not to bias the linearity. Only the most energetic central cells are used for the time measurement, and the time of all the other cells is fixed to this time in the digital filter computation, again to avoid bias on the linearity. In events with several showers, some care has to be taken to subtract the energy leakage from one shower to another, up to shower separation as large as $\approx$ 60 cm, to eliminate small systematic biases in the energy measurement. The measurement of the impact point of the electron or photon is based on the centre of gravity of the shower measured in 3$\times$3 cells, to benefit from the narrow central core of the shower.

4.2 Position resolution

The position resolution has been studied using data taken with a monochromatic electron beam in 1996, by comparing the measured electron shower position to the extrapolated track impact point given by the NA48 spectrometer. The resolution of the later quantity is $\approx 100\mu$m and is negligible compared to the calorimeter resolution. The results achieved are shown in Figure 2, as a function of the electron energy, for both the x (horizontal) and y (vertical) coordinates. The position resolution is better than 1 mm above 25 GeV.

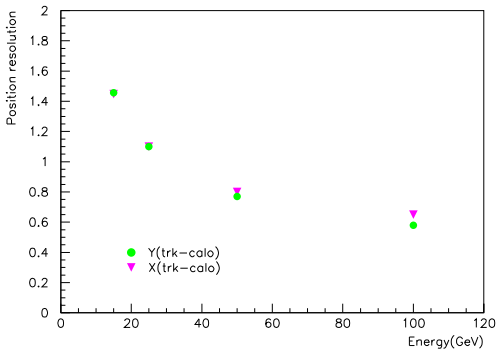

Figure 2: *Position resolution (in mm) as a function of energy, measured with an electron beam.*

4.3 Time resolution

The photon time resolution can be studied using events of the type $K \to 3\pi^0 \to (n)\gamma e^+e^-$, by comparing the photon time to the time of the electron tracks (given by a scintillator array in front of the calorimeter). The time resolution per photon is better than 500 ps. In $K \to \pi^0\pi^0$ events, the final event time is computed combining the time informations from the four photons. The event time resolution is better than 250 ps. The tails outside ± 2 ns are smaller than 10^{-4} level, which is a crucial point for the validity of the K_S/K_L identification method used by NA48 [9].

4.4 Uniformity and energy resolution

4.4.1 Ke3 sample

The main tool to study in situ the detailed performances of the calorimeter is given by a sample of $K_L \to \pi^{\pm} e^{\mp} \nu$ decays (called Ke3 decays), which is very abundant. The electron track can be measured in the spectrometer upstream of the calorimeter. This spectrometer [10] consists of four large drift chambers with a magnet between the second and third chambers (which gives a p_t kick of 265 MeV/c). The position resolution of the drift chambers is better than 100μm. This allows to reconstruct the electron momentum (p) with a resolution given by :

$$\sigma(p)/p = 0.5\% \oplus (0.009\% \times p) \tag{4}$$

where p is expressed in GeV. This measurement of p can be compared to the electron energy E measured with the calorimeter. In an ideal world, the ratio $\frac{E}{p}$ should be 1. Taking p as "perfect", this allows to study the variations in the energy response, the uniformity of the response over the full calorimeter, the energy resolution and the linearity. A total of $\approx 150{\times}10^6$ Ke3 decays were recorded in 1998 and 1999 for this purpose.

4.4.2 Response variation within one cell

Figures 3 show the variation of $\frac{E}{p}$ as a function of the impact point of the electron within one cell. The $\approx$ 0.5% variation with x (horizontal direction) comes from the fact that when the electron shower develops near the anode ($x \approx 0$), the response is slightly reduced because part of the deposited charge drifts during a time smaller than the $\approx$ 70 ns integration time of the shaping. Thanks to the accordion angle, this effect is small and has a smooth variation with the impact point, it can therefore be easily corrected. The drop of the response ($\approx 1\%$) near the vertical separations between cells comes from the fact that in the small vertical gap between two anodes, the electric field is reduced. This variation can also be corrected using the measured shower position. Both these variations can be reproduced by a Monte-Carlo which includes a detailed electric field map, as well as a simulation of the readout electronics. After corrections, the residual variations with the impact point within the cell are $\approx 0.1\%$.

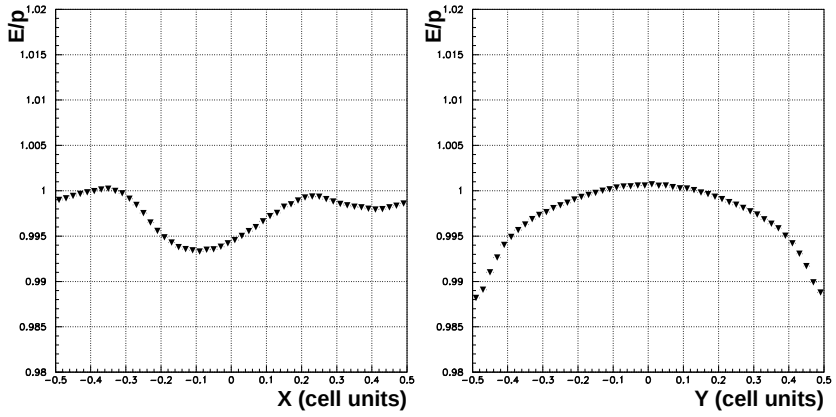

Figure 3: *Variation of E/p as a function of the impact point within the cell in the horizontal (left) and vertical (right) directions.*

4.4.3 Intercalibration

The uniformity of the response over the full calorimeter is studied by computing the average value of $\frac{E}{p}$ per cell (of the maximum energy deposition of the shower). Using only the electronic calibration, and the values of κ measured as described above, the RMS dispersion of $< \frac{E}{p} >$ is 0.41%. This is well consistent with the expected accuracy in the measurement of κ of $\approx 1\%$, given the fact that $\leq 40\%$ of the shower energy is deposited in the impact cell. To improve the uniformity, Ke3 events are used to equalise $< \frac{E}{p} >$ for all impact cells. A simple iterative procedure is used to obtain cell per cell coefficients [11]. For this procedure, only electrons in the energy range 25 to 40 GeV are used, to avoid possible interplay between non-linearity and non-uniformity. This gives intercalibration factors which are one static factor per cell, equivalent to a redefinition of the κ constants. Applying to the 99 Ke3 data the intercalibration factors derived from the 98 Ke3 sample, the RMS dispersion of $< \frac{E}{p} >$ as a function of the impact cell becomes $\approx 0.15\%$, showing the stability of the intercalibration procedure (part of this dispersion is directly coming from the event statistic used in 98 to derive the intercalibration factors). The validity of this procedure is also checked using photons produced in π^0 and η decays,

produced with π^- beam striking thin targets during special runs. The long range uniformity is found to be better than $\approx 0.1\%$.

4.4.4 Energy resolution

From the observed $\frac{E}{p}$ resolution, the energy resolution can be deduced unfolding the momentum resolution. Figure 4 shows the $\frac{E}{p}$ and E resolutions in the Ke3 sample collected in 99, after the intercalibration procedure described above. Because of the different zero suppression scheme used for Ke3 events and $K \to \pi^0\pi^0$ events, the energy measurement in Ke3 events is based on 7×7 calorimeter cells.

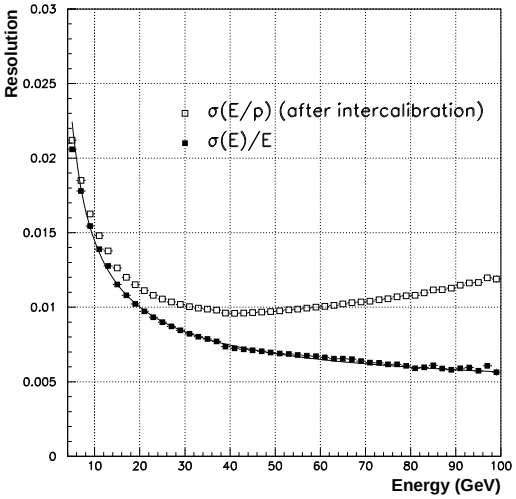

Figure 4: *Resolution on E/p and on E, after unfolding the momentum resolution, as a function of the electron energy, using the Ke3 sample collected in 99.*

The corresponding energy resolution extrapolated to the full shower size used for photons is :

$$\sigma(E)/E = (3.2 \pm 0.2)\%/\sqrt{E} \oplus (0.09 \pm 0.01)/E \oplus (0.42 \pm 0.05)\% \qquad (5)$$

where E is in GeV. The uncertainties quoted include uncertainties in the momentum resolution and in the extrapolation to the full shower size. Above 20 GeV, the energy resolution is better than 1%. At the average energy of 25 GeV, the dominant term in the energy resolution is the sampling term. The coherent noise contribution to the total noise of $\approx$ 90 MeV is almost negligible.

Several effects are expected to contribute to the observed constant term : a GEANT based simulation gives a constant term of $\approx$ 0.2% (residual impact point variations, fluctuations in longitudinal shower development, ...); the intercalibration accuracy is $\approx$ 0.15%, the gap size variations ($\pm$45 μm) should give a constant term contribution of $\approx$ 0.1 to 0.2%; the pulse reconstruction has a $\approx$ 0.1% accuracy in calibration events, and because the physics signal shape is slightly different from calibration, one expects an additional $\approx$ 0.15% constant term contribution. These effects can account qualitatively for the constant term observed in the data, and this shows that there is not one single dominant contribution to the residual constant term. If one did not use the Ke3 intercalibration, the constant term would increase to $\approx$ 0.6%.

The resolution quoted above is the result of a gaussian fit. Some non-gaussian tails are present in the energy response : $\approx$ 1% of the showers have a measured energy lower by more than 3σ from the average value, with $\approx$ 0.1% having a response 20% or more lower. This tail can be interpreted as coming from $\pi^{\pm}$ production in electromagnetic showers through hadronic photoproduction.

4.5 Linearity

The average value of $\frac{E}{p}$ as a function of the electron momentum is shown in Figure 5, where 45 MeV has been added to the electron energy to account for energy loss before the Liquid Krypton. The energy response is linear in the energy range 5-100 GeV within $\approx$ 0.1%. This figure also shows the expectation from Monte-Carlo, which has a small $\approx$ 0.05% non linearity coming from the gap opening : as the energy increases, the shower develops later in the calorimeter at a place where the gap is larger and therefore the initial current smaller. The small structure visible in the data at $E \approx 30$ to 50 GeV is probably coming from a small non linearity in the ADC.

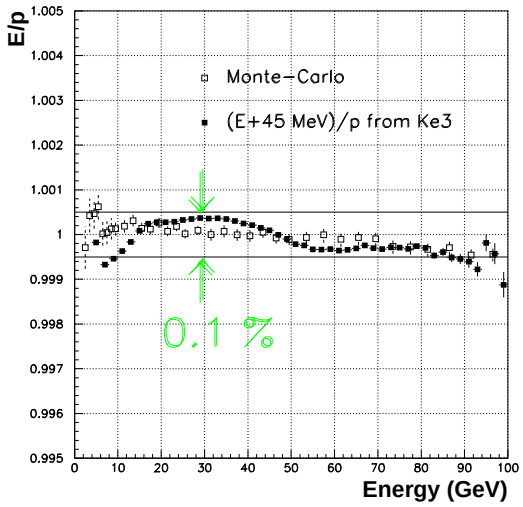

Figure 5: *Average value of E/p as a function of the energy, showing the linearity of the response, for the Ke3 sample collected in 99.*

5 $K \to \pi^0\pi^0$ events and overall energy scale

The resolution of the π^0 mass in $K \to \pi^0\pi^0$ events observed in the data is ≈ 1 MeV, consistent with the expectations based on the energy and position resolutions described above. Thanks to this very good resolution, the level of residual $K \to 3\pi^0$ background is smaller than 0.1% and induces a negligible systematic uncertainty in the measurement of ϵ'/ϵ.

As discussed in the introduction, the decay region definition relies on the measured photon energies and positions: the distance between the reconstructed decay vertex position and the calorimeter is for instance directly proportional to the calorimeter energy scale. Systematic effects from non linearity are small as shown from the Ke3 analysis. One is then only left with fixing the overall energy scale factor of the calorimeter. Given the small difference in electron/photon response from the dead matter before the calorimeter, this is done using the $K \to \pi^0\pi^0$ events themselves. In the K_S beam, an anti-counter located at the beginning of the decay region (122 m upstream of the

calorimeter) is used to sharply define its beginning, by vetoing decays occurring upstream. The calorimeter energy scale is adjusted such that the corresponding sharp rise in the reconstructed decay vertex position matches the known geometrical position of this counter with respect to the calorimeter. This is done with an accuracy of few 10^{-4}. As a cross-check of non linearity, one can check that this factor is constant with the kaon energy (in the range 70-170 GeV) to better than 5×10^{-4}.

6 Conclusions

The performances of the NA48 liquid Krypton calorimeter have been studied extensively in situ. The resolutions achieved ($\approx$ 500 ps time resolution per photon, better than 1 mm position resolution above 25 GeV, better than 1% energy resolution above 20 GeV with a constant term smaller than 0.5%), together with the small non linearity in the energy response and the good stability of the calorimeter over several years, match the requirements for a precise measurement of direct CP violation in the neutral kaon system.

References

1. V. Fanti *et al.*, Phys. Letters B **465**, 335 (1999).
2. The Moliere radius is computed according to the PDG parameterisation : R_M = X0$\times$(21 MeV)/Ec with Ec = 610 MeV/(Z+1.24).
3. C. Cerri in : A. Antonelli *et al.*, Proc. VI Int. Conf. on Calorimetry in HEP, Frascati Physics Serie 6, p 841 (1996).
4. G. Martin-Chassard *et al.*, in : A. Antonelli *et al*, Proc. VI Int. Conf. on Calorimetry in HEP, Frascati Physics Serie 6, p 799 (1996).
5. B. Hallgren *et al.*, Nucl. Instr. Meth. A **419**, 623 (1998).
6. S. Guidici, to appear in the same proceedings.
7. S. Palestini *et al.*, Nucl. Instr. Meth. A **421**, 75 (1999).
8. CERN Program Library Long Writeup W5013, 1993.
9. S. Crépé, thèse, LAL 98-34, Orsay, may 1998.
10. D. Dédérède *et al.*, Nucl. Instr. Meth. A **367**, 88 (1995).
11. J. Ocariz, thèse, LAL 99-24, Orsay, may 1999.